

A Determination of Screening Constants for Incomplete Atomic Shells of Elements $Z=2$ to 23 from Experimental Ionization Potentials—X-ray Photoelectric Mass Absorption Coefficients for Elements $Z=6$ to 15 for 33 Characteristic Energies between 1 and 25 keV

J. D. Stephenson

Fritz-Haber-Institut der Max-Planck-Gesellschaft, Berlin-Dahlem, Germany

(Z. Naturforsch. 31 a, 887—897 [1976]; received June 16, 1976)

A method is proposed, which primarily determines screening constants for *incomplete* atomic shells from the experimental ionization potentials of spin-paired Pauli-type orbitals.

The method is complimentary and in addition to the standard Sommerfeld approach, which derives screening constants from X-ray spin doublet term differences.

Atomic photoelectric absorption cross sections are computed from screened hydrogen-like eigenfunctions for low atomic number elements $Z=6$ to 15, using a range of incident photon energies between 1 and 30 keV. Comparison with experiment and alternate more exact theories shows, that improved cross sections are obtained for the more important incomplete L-shell contributions.

X-ray photoelectric mass absorption coefficients for low Z elements ($Z=6$ to 15), employing 33 characteristic X-ray energies {NiK α (0.852 keV) to AgK β (24.942 keV)}, are given.

1. Introduction

The primary aim of this paper is to determine screening constants for incomplete atomic shells from the successive ionization potentials of each element. Such constants cannot be determined by the standard Sommerfeld method¹, due to the absence of the requisite experimental X-ray spin doublet terms.

This difficulty has already been pointed out in former papers^{2,3}, in which the screening constants of incomplete shells were necessary for the computation of atomic photoelectric absorption cross sections, using hydrogen-like eigenfunctions. In the latter calculations the *incomplete* L, M and N-shell screening constants were taken from *averages* of the calculable full shell values.

This approximation was shown in⁴ to produce cross sections which are relatively poor compared with those obtained from more rigorous Hartree-Fock-Slater theory⁵. Although the contribution of incomplete shell cross sections to the total is less than 1% for elements with atomic numbers $Z>10$, more exact theory⁵ shows that the incomplete L-shell contribution can be of the order of 5% in cases where $Z \cong 6$.

Improved L-shell screening constants are therefore important for the determination of hydrogen-

like photoelectric atomic absorption cross sections of low Z elements from which more accurate X-ray linear and (minimum) anomalous absorption coefficients and associated constants can be estimated.

The following method shows that it is possible to obtain a logical set of sub-shell screening constants for each element from their successive experimental ionization potentials.

2. Method

Atomic sub-shell screening constants were previously determined for low atomic number elements $Z=3$ to 14 by Pauling and Sherman⁶, using *single* ionization potentials. Their use in hydrogen-like atomic photoelectric absorption cross section calculations however does not give values in good agreement with those estimable from X-ray linear absorption measurements, nor with those of more rigorous alternate theories. A similar approach by Bethe and Salpeter⁷ and also by Eisenlohr and Müller⁸ gave the non-relativistic ionization potential $I(n, l)$ of an electron in a sub-shell with quantum numbers n and l in the form

$$I(n, l) = E(n, l) - 2 V_0(n, l) \text{ Ryd.} \quad (1)$$

This relation is derived from the one-electron solution to the Schrödinger equation, in which $E(n, l)$ is the hydrogen-like eigenvalue of the electron state and $V_0(n, l)$ the static potential, produced at small distances external to the shell. For the many electron atom the nuclear charge $+Ze$ is replaced by

Reprint requests to Dr. J. D. Stephenson, Fritz-Haber-Institut der Max-Planck-Gesellschaft, Faraday-Weg 4–6, D-1000 Berlin 33 (Dahlem).



Dieses Werk wurde im Jahr 2013 vom Verlag Zeitschrift für Naturforschung in Zusammenarbeit mit der Max-Planck-Gesellschaft zur Förderung der Wissenschaften e.V. digitalisiert und unter folgender Lizenz veröffentlicht: Creative Commons Namensnennung-Keine Bearbeitung 3.0 Deutschland Lizenz.

Zum 01.01.2015 ist eine Anpassung der Lizenzbedingungen (Entfall der Creative Commons Lizenzbedingung „Keine Bearbeitung“) beabsichtigt, um eine Nachnutzung auch im Rahmen zukünftiger wissenschaftlicher Nutzungsformen zu ermöglichen.

This work has been digitalized and published in 2013 by Verlag Zeitschrift für Naturforschung in cooperation with the Max Planck Society for the Advancement of Science under a Creative Commons Attribution-NoDerivs 3.0 Germany License.

On 01.01.2015 it is planned to change the License Conditions (the removal of the Creative Commons License condition “no derivative works”). This is to allow reuse in the area of future scientific usage.

a reduced charge $+ \{Z - s(n, l)\} e$, in which $s(n, l)$ is considered as the inner screening constant, and where the eigenvalue of the electron state is given by:

$$E(n, l) = \{Z - s(n, l)\}^2 / n^2 \text{ Ryd}^*.$$

$V_0(n, l)$ was alternatively considered as the outer sub-shell screening constant, which for light elements, especially for the outer electrons, is relatively unimportant.

In the following discussion we are primarily concerned with these cases, i.e. the outer K-, L-, M- and N-shells of low Z elements, in which $V_0(n, l)$ is considered negligibly small^{**}. An additional constant, $\pm \Delta E(n, l)$, is however introduced to account for the resultant repulsive energy, experienced by each paired-spin electron in a Pauli-type orbital, when one is removed to the continuum by an ionization process. In such a transition it is presumed that the ejected electron gains energy $+\Delta E(n, l)$ due to the repulsion from the remanent electron, which simultaneously relaxes closer to the nucleus by losing an equivalent amount $-\Delta E(n, l)$. These

events are shown in Fig. 1, where the first ejected electron requires an ionization potential $I_1(n, l)$ plus the repulsive energy $+\Delta E(n, l)$ for its complete escape. The second electron meanwhile relaxes closer to the nucleus by losing energy $-\Delta E(n, l)$, from which state it needs the larger ionization potential $I_2(n, l)$ for its removal. Equation (1) can now be rewritten in the forms

$$I_1(n, l) = E(n, l) - \Delta E(n, l) - \{2 V_0(n, l) \cong 0\} \quad (2a)$$

for the first ionization and

$$I_2(n, l) = E(n, l) + \Delta E(n, l) - \{2 V_0(n, l) \cong 0\} \quad (2b)$$

for the second.

From these equations

$$E(n, l) = \{I_1(n, l) + I_2(n, l)\} / 2 \quad (3)$$

gives the eigenvalue of the two paired-spin electrons before ionization and

$$|\Delta E(n, l)| = \{I_2(n, l) - I_1(n, l)\} / 2 \quad (4)$$

the relaxation energy involved. Substituting $E(n, l)$, determined from Eq. (3), into the Bohr relation leaves all quantities known, except that of the inner screening constant $s(n, l)$.

As a practical example, consider the simplest case for the double ionization of the two paired-spin electrons in the K-shell of a neutral Helium atom. Although the initial eigenvalues of the electrons are identical, two quite different ionization potentials, $I_1(1, 0) = 24,481 \text{ eV}$ and $I_2(1, 0) = 54,403 \text{ eV}$, are required for their removal. Following the procedure outlined above, the initial eigenvalue of the electrons is $E(1, 0) = 39.442 \text{ eV}$, which gives $s(1, 0) = 0.297$ for the K-shell screening constant of a Helium atom. This is in very close agreement with the generally accepted value $s(1, 0) = 0.3$, given empirically by Slater⁹ and used for all K-shells in previous calculations^{2, 3}. Further, if we substitute $I_1(1, 0)$ and $I_2(1, 0)$ into Eq. (4), we obtain $|\Delta E(1, 0)| = 14.96 \text{ eV}$ for the resultant repulsive energy between the two electrons during the *first* ionization event.

Similar determinations of $s(1, 0)$ are possible for the K-shells of elements $Z = 2$ to 8, for which the experimental ionization potentials are available. Their values are remarkably consistent and close to the Slater K-shell value. They are given in Table 1 together with those computed for the higher L_I, L_{II} ,

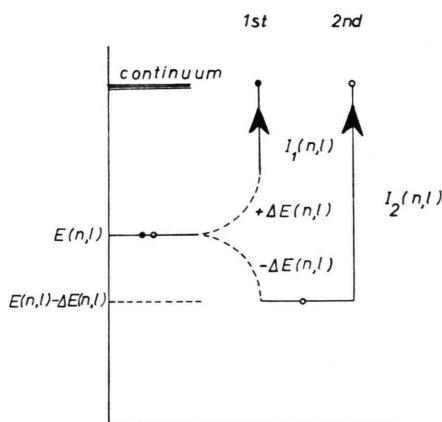


Fig. 1. Grottrian-type diagram showing the relative change in eigenvalue of the two paired-spin electrons in a Pauli-type orbital during successive ionizations. $I_1(n, l)$ and $I_2(n, l)$ are the first and second ionization potentials. $\pm \Delta E(n, l)$ represents the gain or loss in energy of each electron by mutual repulsion during the *first* ionization event.

* $E(n, l)$, used here, is the Bohr relation which is only approximately true for low Z elements. The more exact form, given by Sommerfeld:

$$E(n, l) = [\{Z - s(n, l)\}^2 / n^2 + \{Z - s(n, l)\}^4 \alpha^2 (n/l - 3/4) / n^4] \text{ Ryd},$$

where $\alpha = 7.298 \cdot 10^{-3}$, is important for the higher Z elements for which $(\alpha Z)^2 \gg 1$.

* For medium-heavy and heavy atoms, especially for inner electrons, $V_0(n, l)$ is quite large and cannot be neglected in this context.

Table 1. Computed ionization potential screening constants $s(n, l)$ for the outer paired-spin orbitals of elements $Z=2$ to 23. Bracketed values are determined for single unpaired-spin electrons.

	1s	2s	2p			3s	3p			3d					4s
	K _I	L _I	L _{II}	L _{III}		M _I	M _{II}	M _{III}		M _{IV}	M _V				N _I
<i>n, l</i>	1,0	2,0	2,1			3,0	3,1			3,2					4,0
<i>j</i>	1/2	1/2	1/2	3/2	3/2	1/2	1/2	3/2	3/2	3/2	3/2	5/2	5/2	5/2	1/2
No el	(2)	(2)	(2)	(2)	(2)	(2)	(2)	(2)	(2)	(2)	(2)	(2)	(2)	(2)	(2)
<i>Z</i>															
1	0	—	—	—	—	—	—	—	—	—	—	—	—	—	—
2	0.297	—	—	—	—	—	—	—	—	—	—	—	—	—	—
3	0.301	(1.73)	—	—	—	—	—	—	—	—	—	—	—	—	—
4	0.305	1.99	—	—	—	—	—	—	—	—	—	—	—	—	—
5	0.306	1.95	(3.44)	—	—	—	—	—	—	—	—	—	—	—	—
6	0.307	1.94	3.71	—	—	—	—	—	—	—	—	—	—	—	—
7	0.306	1.92	3.63	(4.93)	—	—	—	—	—	—	—	—	—	—	—
8	0.306	1.91	3.59	5.32	—	—	—	—	—	—	—	—	—	—	—
9	—	1.91	3.56	5.21	(6.74)	—	—	—	—	—	—	—	—	—	—
10		—	3.54	5.14	6.96	—	—	—	—	—	—	—	—	—	—
11		1.89	3.52	5.09	6.82	(9.16)	—	—	—	—	—	—	—	—	—
12		1.89	3.50	5.06	6.72	9.26	—	—	—	—	—	—	—	—	—
13		1.88	3.49	5.03	6.66	9.04	(11.0)	—	—	—	—	—	—	—	—
14		1.88	3.48	5.01	6.61	3.90	11.2	—	—	—	—	—	—	—	—
15		1.87	3.47	4.99	6.57	8.80	10.9	(12.4)	—	—	—	—	—	—	—
16		—	—	4.98	6.53	8.71	10.8	12.7	—	—	—	—	—	—	—
17		—	—	4.96	6.51	8.64	10.7	12.4	(14.1)	—	—	—	—	—	—
18			—	—	—	8.59	10.6	12.3	14.2	—	—	—	—	—	—
19						8.54	10.5	12.1	13.9	—	—	—	—	—	(16.7)
20						8.51	10.5	12.0	13.8	—	—	—	—	—	16.8
21						8.45	10.4	11.9	13.6	(18.9)	—	—	—	—	16.3
22						8.42	10.4	11.8	13.5	(19.0)	(19.9)	—	—	—	15.6
23						8.39	—	—	13.4	(18.6)	(19.9)	(20.9)	—	—	14.9

Averaged Sommerfeld screening constants used by HSW³

1s	2s, 2p	3s, 3p	3 d	4s
0.3	3.22	8.20	12.9	18.5

Table 2. Relaxation energies $|\Delta E(n, l)|$, in eV, for each sub-shell of elements $Z=2$ to 23, computed from experimental Ionization potentials. The average increment in $|\Delta E(n, l)|$ for each sub-shell, as Z increases, is given at the bottom of each column.

	1s K	2s L _I	L _{II}	2p L _{III}		3s M _I	M _{II}	3p M _{III}		3d M _{IV}		M _V			4s N _I
n, l	1,0	2,0		2,1		3,0		3,1		3,2					4,0
j	1/2	1/2	1/2	3/2	3/2	1/2	1/2	3/2	3/2	3/2	3/2	5/2	5/2	5/2	1/2
No el.	(2)	(2)	(2)	(2)	(2)	(2)	(2)	(2)	(2)	(2)	(2)	(2)	(2)	(2)	(2)
Z															
1	0														
2	14.96														
3	23.40	0													
4	31.90	4.44													
5	40.41	6.39	0												
6	46.93	8.30	6.56												
7	57.45	10.21	8.92	0											
8	66.00	12.10	11.25	10.75											
9	—	14.01	13.54	13.83	0										
10	—	—	15.80	16.76	9.76										
11	—	—	18.18	19.75	12.21	0									
12	—	—	20.53	22.63	14.58	3.69									
13	—	—	—	25.48	16.90	4.81	0								
14	—	—	—	28.33	19.19	5.82	4.10								
15	—	—	—	31.17	21.45	6.83	5.22	0							
16	—	—	—	34.05	23.90	7.76	6.14	6.52							
17	—	—	—	37.80	26.20	8.79	7.15	8.05	0						
18	—	—	—	—	—	9.73	8.15	9.45	5.93						
19	—	—	—	—	—	—	9.15	10.85	7.10						0
20	—	—	—	—	—	—	7.65?	12.30	7.90						2.88
21	—	—	—	—	—	—	—	14.00	9.05	0					5.98
22	—	—	—	—	—	—	—	15.50	10.10	0	0				7.89
23	—	—	—	—	—	—	—	—	11.00	0	0	0	—	—	8.50
Average increment in $ \Delta E(n, l) $ for each sub-shell with increasing atomic number Z .															
	8.50	1.91	2.33	2.93	2.36	1.00	1.03	1.50	1.01	—	—	—	—	—	?

L_{III}, \dots, N_I sub-shells of elements $Z = 2$ to 23. The corresponding relaxation energies $|\Delta E(n, l)|$ are given in Table 2.

Ionization potentials, required in these calculations, are taken from published vacuum ultraviolet spectrometry measurements¹⁰, and used in conjunction with the known electronic configuration of each element. The outermost (lowest ionization potential) sub-shells are considered first. In specific cases, where the outer sub-shell of a neutral atom has only one unpaired electron, $s(n, l)$ is calculated directly from Eq. (2b), in which $\Delta E(n, l)$ is taken to be zero, since it has no meaning in this case. Approximated Sommerfeld screening constants, used earlier³ for incomplete sub-shells, are given for comparison at the bottom of each column in Table 1.

Atomic photoelectric absorption cross section formulae, employing the ionization potential screening constants derived in this paper, are taken from several sources, which have been conveniently listed by

Wagenfeld¹¹. These calculations employ non-relativistic screened hydrogen-like eigenfunctions. The Slater screening constant for the K-shell, $s(1, 0) = 0.3$, is retained for each element together with the theoretical extension to the K-shell described in³.

3. Discussion

3.1. Screening Constants

Figure 2 shows that the ionization potential screening constants of each Pauli-type orbital, determined from the method outlined above and given in Table 1, are sensibly consistent in reaching a maximum at each complete 2-electron value and thereafter decreasing monotonically as each new sub-shell is formed. The resolution of screening constant is superior to that obtained from the Som-

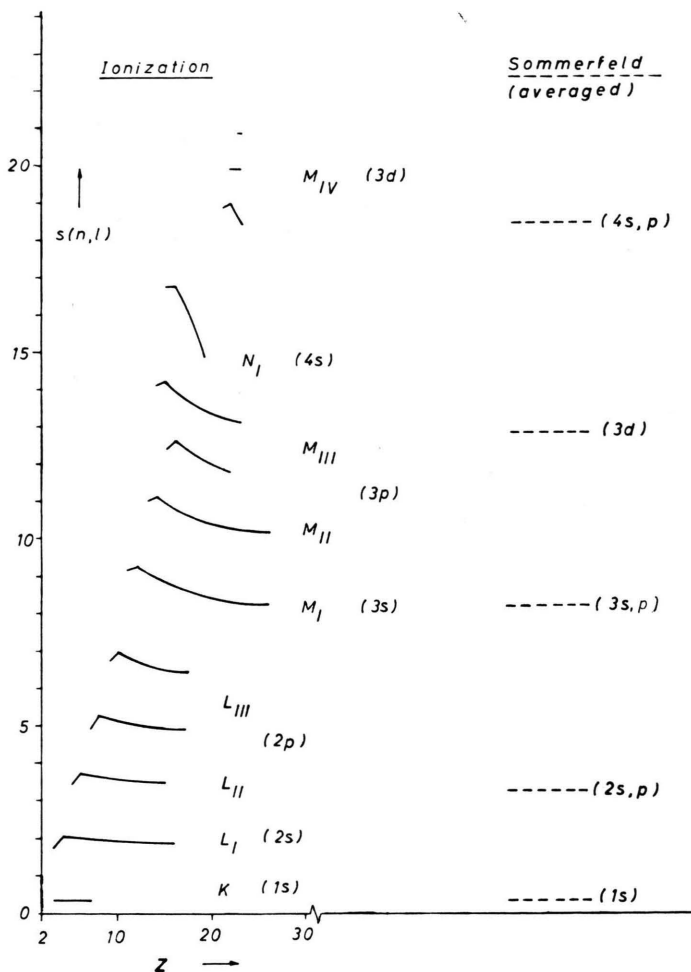


Fig. 2. The variation in ionization potential screening constant $s(n, l)$ of each paired-spin Pauli-type orbital (full lines) for elements $Z=2$ to 23. Averaged Sommerfeld screening constants, used in former calculations³ for incomplete sub-shells, are given on the right-hand side (dashed lines).

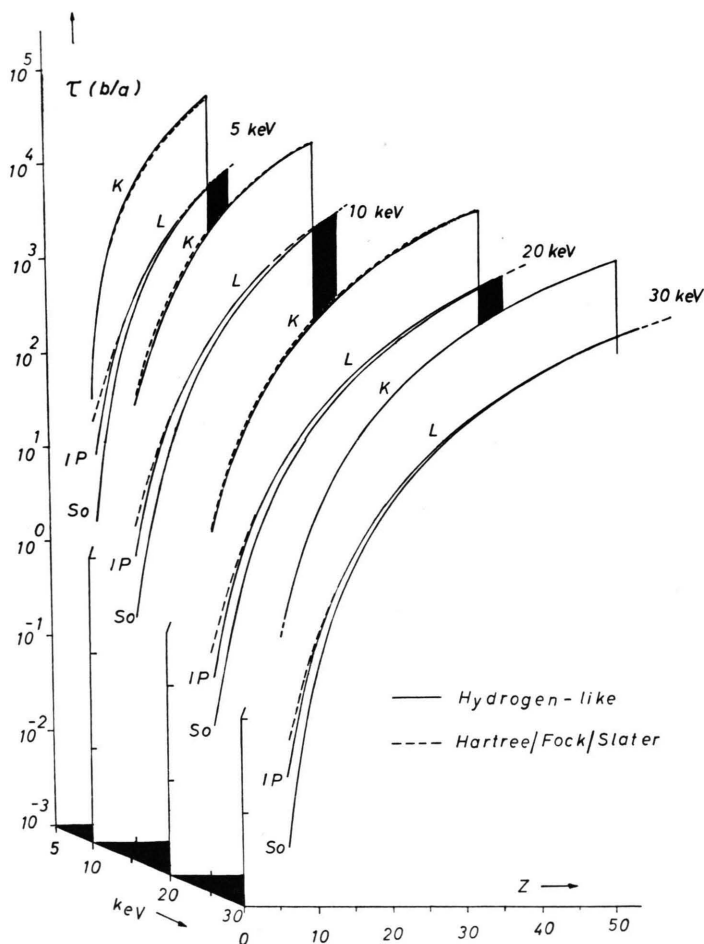


Fig. 3. Superimposed K- and L-shell atomic absorption cross section profiles for low atomic number elements, using incident photon energies 5, 10, 20 and 30 keV. The photoeffect cross sections τ , in barn/atom, are computed from screened hydrogen-like formulae, using both IP — ionization potential and So — averaged Sommerfeld screening constants (full lines). They are contrasted with similar results, calculated by Scofield⁵, from more exact theory (dashed lines). The figure shows that closer agreement is obtained between the total L-shell cross sections of the ionization potential method and those of Scofield than was obtained from averaged Sommerfeld screening constants³. (Note: Each pair of K- and L-shell profiles has a different $Z=0$ origin along the keV axis.)

merfeld approach. The figure also shows that the new L_I -shell screening constants are lower and the L_{III} -shell constants higher than the corresponding averaged (2s, 2p) Sommerfeld screening constants used in earlier calculations³. These differences cause relatively important changes in the photoelectric absorption cross sections obtained from screened hydrogen-like eigenfunctions. They are especially effective for the low Z elements ($Z \cong 6$), where the L-shell contribution to the total is of the order of 5%.

For example, the lower L_I -shell (2s) ionization potential screening constants for these elements will tend to raise the absorption cross sections of these shells, relative to those obtained earlier³, and bring them into closer coincidence with those of the more exact Hartree-Fock Slater theory^{5, §}. Conversely, the

higher L_{III} -shell ionization potential screening constants will give lower cross sections, which are more important for medium to heavy elements. The relative changes in absorption cross section for the latter elements will therefore be more noticeable near an L-shell absorption edge and should again tend to improve those cross sections of former calculations³ near these edges.

3.2. Hydrogen-like Photoelectric Atomic Absorption Cross Sections

The changes in incomplete L-shell cross sections of low Z elements, brought about by using the new ionization potential screening constants, are shown in Fig. 3 for incident photon energies 5, 10, 20 and 30 keV. The full lines in these diagrams are for screened hydrogen-like cross sections, using both the ionization potential (IP) and averaged Sommerfeld (So) screening constants. The dashed lines

§ A similar, though less resolved, distribution in screening constant values was also reported by Duncanson and Coulson¹².

Table 3. Sub-shell *photoelectric* absorption cross sections τ , in barn/atom, for elements $Z=6$ to 10, computed from screened hydrogen-like eigenfunctions, using the ionization potential screening constants determined in this work. They are compared with the photoionization cross sections of Scofield⁵ and Storm and Israel¹³, using more exact theory and incident photon energies 1, 5, 10, 20 and 30 keV.

keV		1.0				5.0				10.0			
Z	K	L _I	L _{II} , L _{III}	Total	K	L _I	L _{II} , L _{III}	Total	K	L _I	L _{II} , L _{III}	Total	
C 6	40390	1210	2.08	41602	315.8	8.66	2.3–3	324.5	35.18	0.93	1.17–4	36.11	
	42045	2028	—	44073	353.9	18.2	—	372.1	39.3	2.0	—	41.3	
N 7	73102	2804	22.67	75929	627.9	22.97	3.0–2	650.9	71.97	2.56	1.58–3	74.53	
	—	—	—	76600	—	—	—	717	—	—	—	78.8	
O 8	119258	5326	113.6	124698	1120	49.29	1.7–1	1170	131.9	5.70	9.5 –3	137.6	
	—	—	—	121000	—	—	—	1250	—	—	—	142	
F 9	180102	8926	398.2	189427	1844	92.5	6.9–1	1937	222.6	11.07	3.9 –2	233.7	
	—	—	—	179000	—	—	—	2030	—	—	—	246	
Ne 10	256544	13669	1099	271312	2849	157.3	3.86	3009	352.3	19.46	2.6 –1	372	
	232060	16051	—	248111	2924	171.0	—	3095	362	21.0	—	383	
	—	—	—	252000	—	—	—	3100	—	—	—	386	
	—	—	—	—	—	—	—	—	—	—	—	—	

keV		20.0				30.0				
Z	K	L _I	L _{II} , L _{III}	Total	K	L _I	L _{II} , L _{III}	Total	Ref.	
C 6	3.788	9.7–2	5.93–6	3.89	1.023	2.52–2	1.05–6	1.048	This work S	
	4.1	0.2	—	4.3	1.081	5.71–2	—	1.138		
N 7	7.93	2.75–1	8.23–6	8.20	2.164	7.40–2	1.47–5	2.238	This work S&I	
	—	—	—	8.51	—	—	—	2.27		
O 8	14.85	6.29–1	5.11–4	15.48	4.097	1.71–1	9.28–6	4.268	This work S&I	
	—	—	—	15.7	—	—	—	4.23		
F 9	25.58	1.254	2.16–3	26.84	7.13	3.46–1	3.98–4	7.476	This work S&I	
	—	—	—	26.8	—	—	—	7.27		
Ne 10	41.29	2.263	1.60–2	43.57	11.62	6.32–1	3.20–3	12.26	This work S S&I	
	41.6	2.4	—	44.0	11.38	6.62–1	—	12.04		
	—	—	—	42.9	—	—	—	11.8		

indicate the photoionization cross sections of Scofield⁵, using the more exact Hartree-Fock-Slater theory. The figure shows that the cross sections, computed from the ionization potential screening constants, are now in closer agreement with Scofield than obtained earlier³, using averaged Sommerfeld screening constants.

Specific cross sections for the K-, L_I- and L_{II}, L_{III}-shells are given in Table 3 for elements $Z=6$ to 10. They are compared with the more rigorous K- and L-shell cross sections of Scofield⁵ and Storm and Israel¹³ for incident photon energies 1, 5, 10, 20 and 30 keV. For $Z>6$ most total cross sections are well within a 5% difference; those for $Z=6$ are variable and can differ by 13% at 5 keV. The total L-shell cross sections for carbon are approximately

half those given by Scofield, for all energies considered. These difference however diminish rapidly as Z increases until the L-shell cross sections at $Z=10$ are within 8% at 1 keV, decreasing to 4% at 30 keV.

In the special case of aluminium, $Z=13$, more detailed information concerning the L_I-, L_{II}- and L_{III}-shell cross sections is available from several alternate theoretical sources^{5, 13–17}. They are given in Table 4 for photon energies 1, 5, 10 and 30 keV together with those of this and former work⁴. The table shows that a definite improvement in L-shell cross section, compared to those of the more exact theories, is obtainable from the ionization potential screening constants than was possible using averaged Sommerfeld constants.

Table 4. Sub-shell *photoelectric* absorption cross sections τ , in barn/atom, for aluminium, $Z=13$, computed from screened hydrogen-like eigenfunctions, using a) ionization potential screening constants (this work) and b) *averaged* Sommerfeld screening constants (HSW³). Those computed from more rigorous alternate theories are also given by S — Scofield⁵, RR — Rakavy and Ron¹⁴, SP — Schmickley and Pratt¹⁵, BZ — Brysk and Zerby¹⁶ and MC — Manson and Cooper¹⁷. Bracketed H-like values are doubtful; bracketed alternate theory values are taken from¹³.

Al ($Z=13$)	1s K	2s L_I	LII	2p $2,1$	LIII	Total L	3s M_I	3p M_{II}	Total τ	Ref.
n, l	1,0	2,0					3,0	3,1		
j	1/2	1/2	1/2	3/2	3/2		1/2	1/2		
No el.	(2)	(2)	(2)	(2)	(2)	(8)	(2)	(1)		
keV										
1.0	—	34693	6502	2693	813.4	44701	319.8	9.64	45031	This work
	—	24580	—	23040	—	47620	(689.2)	—	48310	HSW
	—	—	—	—	—	51060	—	19.41	53000	S
	—	22750	7152	—	14070	43972	—	—	(44000)	RR
5.0	8040	525.7	17.98	6.38	1.60	551.7	2.279	0.014	8594	This work
	8040	333.8	—	65.69	—	(399.5)	—	(5.364)	8445	HSW
	7996	—	—	—	—	581.4	—	33.86	8611	S
	7862	430.2	27.96	—	54.65	512.8	—	—	(8380)	RR
10.0	1063	71.2	1.19	0.40	0.095	72.86	0.24	7.4—4	1136	This work
	1063	37.1	—	3.44	—	47.9	—	(0.32)	1111	HSW
	1020	68.6	2.61	—	4.76	75.97	—	—	1100	SP
	1066	67.6	2.63	—	5.07	75.3	—	—	(1150)	BZ
	1064	—	—	—	—	75.16	—	4.81	1146	S
	1036	60.8	2.05	—	3.93	66.78	—	—	(1100)	RR
	1064	67.1	—	—	—	(67.1)	—	—	(1140)	MC
30.0	38.06	2.57	0.014	0.0045	0.001	2.595	0.0066	6.4—6	40.6	This work
	38.06	1.51	—	0.053	—	1.56	—	(0.017)	39.6	HSW
	35.1	2.41	0.035	—	0.063	2.588	—	—	37.8	SP
	36.5	2.49	0.036	—	0.067	2.587	—	—	39.3	BZ
	36.37	—	—	—	—	2.534	—	0.175	39.1	S
	35.2	2.21	0.027	—	0.052	2.289	—	—	(37.5)	RR
	36.2	2.22	—	—	—	(2.22)	—	—	(38.5)	MC

Table 5. Hydrogen-like *photoeffect* linear absorption coefficients τ , in cm^{-1} , for silicon ($Z=14$), computed from a) ionization potential screening constants (this work) and b) *averaged* Sommerfeld screening constants (HSW³). They are compared with those of more recent Hartree-Fock theory by Calamitrou and Filippakis¹⁹ and those determined experimentally by Stiglich et al.²⁰ and Hildebrandt²¹ together with the compiled theoretical/experimental results given in the "International Tables for Crystallography"²². Estimates of other scattering contributions \blacktriangle , to be added with some caution to the theoretical values for comparison with experiment, are obtained from Sano et al.¹⁸.

Line	Theory			\blacktriangle ¹⁸	Experiment		Ex/Th
	HF ¹⁹	HSW ³	H-like This work		²⁰	²¹	
AgK α	7.28	6.94	7.10	0.49	7.61	7.32	7.58
MoK α	14.79	14.25	14.55	0.49	14.7	14.6	15.21
CuK α	144.3	142.9	145.4	0.42	137	144	152.1
CoK α	221.5	220.7	224.4	0.39	214	—	233.8
FeK α	277.2	277.2	281.7	0.37	270	275	293.4
CrK α	445.5	448.2	454.9	0.30	445	—	471.9

Experimentally, the new total atomic absorption cross sections for silicon, $Z=14$, are computed for several characteristic X-ray energies and converted to X-ray *photoelectric* linear absorption coefficients τ in cm^{-1} . Other scattering contributions, due to Compton and thermal diffuse scattering, are esti-

mated from theoretical values given by Sano, Ohtaka and Ohtsuki^{18, *}. Such values are given in Table 5 together with more recent Hartree-Fock calculations¹⁹. *Experimental* linear absorption coef-

* These values are unconfirmed and must be treated with some caution.

ficients for this element, measured by Stiglich et al.²⁰ and Hildebrandt²¹, are also given. The new photo-effect linear absorption coefficients τ in this table are approximately 2% higher than those of former work³, in which averaged Sommerfeld screening constants were employed. They are, in this respect, closer to those recently computed from Hartree-Fock theory¹⁹, and those given in the "International Tables of Crystallography"²².

Photoelectric linear mass absorption coefficients τ/ρ , in cm^{-2}/g , are computed for elements $Z=6$ to 15 for 33 characteristic X-ray energies between NiLa (0.852 keV) and $\text{AgK}\beta$ (24.942 keV). They are given in Table 6 and calculated from screened hydrogen-like eigenfunctions, using the ionization potential screening constants derived in this work. Other coherent and incoherent scattering contributions for these elements can be estimated from the extensive tables given by Viegeler et al.²³. They should be added, with some caution, to the photo-effect values for comparison with experimental linear mass absorption coefficients μ/ρ .

Table 6 is an extension of a similar one, given in earlier paper⁴, which was restricted to elements $Z=10$ to 39 and which employed averaged Sommerfeld screening constants. The ionization potential mass absorption coefficients of Table 6, for $\text{Ne}(10)$ and $\text{Al}(13)$, are generally in closer agreement with those determined experimentally by Wuilleumier²⁴ and Bearden²⁵ (for Ne) and Singman²⁶ and Short et al.²⁷ (for Al) over this soft to medium X-ray energy range.

The latter experimental values, except those of Short et al., were tabulated in⁴. In this respect it is possible that the mass absorption coefficients, listed in Table 6 for the lower Z elements ($Z < 10$), are also closer to those which would be obtained experimentally. This is unconfirmed at present, due to the scarcity of these measurements, especially in the soft X-ray energy region.

3.3. Q -factor used in the Theoretical Determination of Anomalous Absorption Coefficients

The ratios $Q = \tau^Q/\tau$ of the quadrupole contributions τ^Q to the total photoelectric atomic absorption cross sections τ , which are used in the theoretical determination of (minimum) anomalous absorption coefficients of X-rays dynamically diffracted through thick perfect single crystals (Borrmann effect)¹¹, remain almost unaffected by the new ionization po-

tential screening constants. Former calculations³, using the averaged Sommerfeld screening constants, give values of Q for elements $Z=6$ to 54 for 18 characteristic X-ray energies between 5 and 25 keV. In the special case of germanium ($Z=32$) these values for several low order reflections have been found to be sufficiently accurate for most experimental purposes².

3.4. Relaxation Energies $|\Delta E(n, l)|$

$|\Delta E(n, l)|$ energies in eV are given in Table 2 for those Pauli sub-shells that are calculable for elements between $Z=2$ to 23. They are determined from Equation (4).

One immediate feature of these results is the almost linear increase in $|\Delta E(n, l)|$ for each sub-shell as the atomic number increases. For example $|\Delta E(1, 0)|$ for the K-shell increases on average by 8.5 eV for each new element formed, $|\Delta E(2, 0)|$ increases by 1.91 eV for the L_{I} -shell, ... etc. These average increments are given at the bottom of each sub-shell column in Table 2.

The horizontal rows of Table 2 show an oscillatory increase in the $|\Delta E(n, l)|$ value towards the centre of the atom with a final sharp rise at the K-shell. Maxima appear to be located at the K-, L_{III} - and M_{III} -shells and minima at the L_{II} - and M_{II} -shells.

4. Conclusion

The screening constants determined in this paper, show that the ionization potential method is inherently capable of giving a more highly resolved set of sub-shell screening constants than the X-ray spin-doublet term difference method of Sommerfeld.

The full range of ionization potential screening constants calculable is limited by the lack of experimental ionization potentials for the *innermost complete* sub-shells of medium to heavy elements. In this respect the method is complementary to that of Sommerfeld, which is conversely limited by an absence of experimental spin-doublet terms for the *outer incomplete* shells. There is however a sufficient overlapping of results for a comparison to be made between the two approaches.

The higher resolution in screening constants, given here, emphasizes the importance of a weighted distribution in sub-shell screening constant values within each shell. In the case of the incomplete L-shells their contribution to the total produces im-

Table 6. Hydrogen-like *photoeffect* mass absorption coefficient τ/ρ , in cm^2/g , using ionization potential screening constants derived in this work. The calculations are for low atomic number elements $Z=6$ to 15, using 33 characteristic X-ray photon energies between $\text{NiL}\alpha$ (0.852 keV) and $\text{AgK}\beta$ (24.942 keV). Other incoherent and coherent scattering contributions, to be added to the photoeffect values with some caution, can be estimated from the tables given by Viegeler et al.²³.

Line	keV	C(6)*	N(7)	O(8)	F(9)	Ne(10)	Na(11)	Mg(12)	Al(13)	Si(14)	P(15)	cm^2/g
NiL α	0.852	3295	5093	7226	9159	671.8	899.5	1203	1536	2023	2485	K
CuL α	0.930	2568	3997	5708	7277	9771	715.7	957.7	1221	1607	1972	
ZnL α	1.012	2016	3158	4539	5817	7848	573.4	769.9	978.3	1287	1577	
MgK α	1.254	1083	1724	2515	3269	4465	5431	436.6	555.6	730.7	893.2	
AlK α	1.487	656.7	1057	1560	2050	2828	3469	4402	353.2	464.5	567.4	
AlK β	1.557	573.2	925.7	1370	1805	2496	3070	3904	312.3	410.9	501.7	
SiK α	1.739	412.2	670.3	998.9	1325	1844	2281	2915	3443	305.2	373.0	
ZrL α	2.042	255.1	418.9	630.1	843.3	1184	1477	1901	2261	2789	242.1	
MoL α	2.293	179.9	297.4	450.1	606.2	856.2	1074	1390	1662	2059	2354	
SK α	2.307	176.5	291.9	441.9	595.3	841.1	1055	1367	1639	2025	2317	
AgL α	2.984	80.62	135.3	207.5	283.2	405.0	514.4	674.0	814.5	1020	1176	
KK α	3.313	58.44	98.58	152.0	208.5	299.6	382.3	503.0	610.5	767.5	889.1	
SnL α	3.444	51.87	87.66	135.5	186.1	267.9	342.3	451.2	548.4	690.4	800.9	
CaK α	3.690	41.91	71.07	110.2	151.8	219.2	280.9	371.4	452.6	571.3	664.1	
TiK α	4.511	22.44	38.44	60.13	83.58	121.7	157.2	209.4	257.1	326.9	382.9	
CrK α	5.415	12.67	21.87	34.49	48.30	70.82	92.11	123.5	152.6	195.3	230.1	
CrK β	5.947	9.43	16.36	25.89	36.39	53.57	69.87	93.99	116.5	149.5	176.7	
FeK α	6.404	7.47	12.99	20.62	29.07	42.90	56.10	75.66	94.02	120.9	143.2	
CoK α	6.930	5.82	10.15	16.17	22.86	33.83	44.36	59.98	74.72	96.34	114.4	
FeK β	7.058	5.49	9.59	15.28	21.61	32.02	42.00	56.83	70.84	91.38	108.5	
NiK α	7.478	4.57	8.00	12.78	18.11	26.88	35.34	47.90	59.82	77.30	91.97	
CoK β	7.649	4.25	7.45	11.92	16.90	25.11	33.03	44.80	55.98	72.39	86.18	
CuK α	8.048	3.62	6.35	10.18	14.46	21.51	28.35	38.52	48.21	62.43	74.44	
NiK β	8.265	3.36	5.84	9.37	13.33	19.84	26.18	35.59	44.58	57.77	68.93	
ZnK α	8.639	2.89	5.09	8.17	11.63	17.34	22.91	31.20	39.12	50.77	60.65	
CuK β	8.905	2.62	4.62	7.43	10.60	15.81	20.91	28.50	35.77	46.46	55.54	
ZnK β	9.572	2.08	3.68	5.93	8.48	12.69	16.81	22.96	28.88	37.58	45.02	
GeK α	9.886	1.88	3.32	5.36	7.68	11.50	15.25	20.84	26.24	34.18	40.98	
GeK β	10.982	1.34	2.38	3.86	5.54	8.33	11.08	15.19	19.18	25.06	30.12	
MoK α	17.479	0.30	0.54	0.89	1.30	1.98	2.67	3.70	4.73	6.25	7.59	
MoK β	19.608	0.21	0.38	0.62	0.90	1.38	1.87	2.60	3.33	4.41	5.38	
AgK α	22.163	0.14	0.25	0.42	0.61	0.94	1.28	1.79	2.29	3.05	3.72	
AgK β	24.942	0.095	0.17	0.29	0.42	0.65	0.89	1.24	1.60	2.13	2.61	

* Graphite $\rho=2.25 \text{ g/cm}^3$.

improvements in absorption cross sections relative to those of more exact theories. In this respect the application of ionization potential screening constants in screened hydrogen-like cross section formulae is also aesthetically more satisfactory than the use of averaged Sommerfeld (full shell) constants.

Further measurements of the ionization potentials for the inner atomic sub-shell of the low Z elements would be useful in completing the list of the

ionization potential screening constants given in Table 1.

Acknowledgements

My thanks are given to Prof. F. Forstmann, of this Institute and of the Theoretical Physics Department, Freie Universität, Berlin, for an initial discussion concerning the Helium atom and also to Prof. G. Hildebrandt for kindly reading through the manuscript and making several useful suggestions.

- ¹ A. Sommerfeld, *Atombau und Spektrallinien*, Vieweg, Braunschweig 1950, 2nd ed., Vol. 1.
- ² G. Hildebrandt, J. D. Stephenson, and H. Wagenfeld, *Z. Naturforsch.* **28a**, 588 [1973].
- ³ G. Hildebrandt, J. D. Stephenson, and H. Wagenfeld, *Z. Naturforsch.* **30a**, 697 [1975].
- ⁴ J. D. Stephenson, *Z. Naturforsch.* **30a**, 1133 [1975].
- ⁵ J. H. Scofield, U. of Calif. Radn. Lab. Report N° 51326 (1973), unpublished.
- ⁶ L. Pauling and J. Sherman, *Z. Kristallograph* **81**, 1 [1932].
- ⁷ H. A. Bethe and E. E. Salpeter, *Quantum Mechanics of One and Two Electron Systems*, *Encycl. of Physics XXXV*, 1, Springer-Verlag, Berlin 1957.
- ⁸ H. Eisenlohr and G. L. J. Müller, *Z. Physik* **136**, 491, 511 [1954].
- ⁹ J. C. Slater, *Phys. Rev.* **36**, 51 [1930].
- ¹⁰ *Hndbk. of Chem. Phys.*, Weast, 55th Ed., Chem. Rub. C°, E-68 (1974-75).
- ¹¹ H. Wagenfeld, *Phys. Rev.* **144** (1), 216 [1966].
- ¹² W. E. Duncanson and C. A. Coulson, *Proc. Roy. Soc. Edin.* **62**, 37 [1944].
- ¹³ E. Storm and H. J. Israel, *Nuclear Data Tables A* **7**, 565 [1970].
- ¹⁴ G. Rakavy and A. Ron, *Phys. Rev.* **159**, 50 [1967].
- ¹⁵ R. Schmickley and R. Pratt, *Phys. Rev.* **164**, 104 [1967].
- ¹⁶ H. Brysk and C. D. Zerby, *Phys. Rev.* **171**, 292 [1968].
- ¹⁷ S. T. Manson and J. W. Cooper, *Phys. Rev.* **165**, 126 [1968].
- ¹⁸ H. Sano, K. Ohtaka, and Y. H. Ohtsuki, *J. Phys. Soc. Japan* **27**, 1254 [1969].
- ¹⁹ M. Calamiotou and S. E. Filippakis, *J. Physics C; Solid State Phys.* **7** [1974].
- ²⁰ J. Stiglich, R. J. Weiss, and A. M. Hansen, in: *Adinterim Special Comm. on Electron Charge, Spin and Momentum Density*, Watertown, Mass., May 1974.
- ²¹ G. Hildebrandt and J. D. Stephenson, *Z. Naturforsch.* **30a**, 1493 [1975].
- ²² *International Tables for Crystallography*, Vol. IV, The Kynoch Press, Birmingham 1974.
- ²³ W. J. Viegele et al., *X-ray Cross Section Compilations from 0.1 keV to 1 MeV*. Report N° DNA 2433F, Rev. I [1971]. Applications to The Director, Defence Nuclear Agency, Washington D.C., 20305, USA. Recently published in: *Handbook of Spectrometry*, Vol. I, C.R.C. Press, Cleveland 1974.
- ²⁴ F. Wuilleumier, *Phys. Paris* **26**, 776 [1965]; *Phys. Rev.* **6**, 2067 [1972].
- ²⁵ A. J. Bearden, *J. Appl. Phys.* **4**, 1681 [1966].
- ²⁶ L. Singman, *J. Appl. Phys.* **45** (4), 1885 [1974].
- ²⁷ M. A. Short and J. Tabock, *X-Ray Spectrometry* **4**, 119 [1975].